

Electronic Supplementary Information
for
On the photophysical properties of Ir^{III}, Pt^{II},
and Pd^{II} (phenylpyrazole) (phenyldipyrrin)
complexes

Jelena Föller,[†] Daniel H. Frieze,[†] Stefan Riese,[‡] Jeremy M. Kaminski,[†] Simon
Metz,[†] David Schmidt,[¶] Frank Würthner,[¶] Christoph Lambert,[‡] and Christel M.
Marian^{*,†}

[†]*Institut für Theoretische Chemie und Computerchemie, Heinrich-Heine-Universität
Düsseldorf, Universitätsstr. 1, 40225 Düsseldorf, Germany*

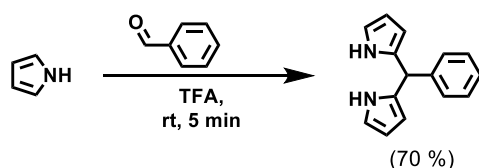
[‡]*Institut für Organische Chemie, Julius-Maximilians-Universität Würzburg, Am Hubland,
97074 Würzburg, Germany*

[¶]*Institut für Organische Chemie and Center for Nanosystems Chemistry (CNC),
Julius-Maximilians-Universität Würzburg, Am Hubland, 97074 Würzburg, Germany*

E-mail: Christel.Marian@hhu.de

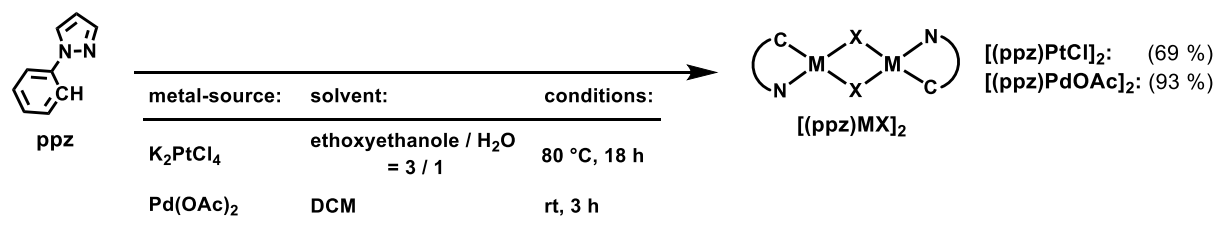
Synthesis

As shown in **Scheme S1**, the first step in the synthesis of the ligand precursor **5-phenyldipyrromethane** was the acid catalyzed condensation of two equivalents of pyrrole with one equivalent of benzaldehyde. In this reaction introduced by *Lindsey et al.*, pyrrole is used not only as a reactant but also as the solvent. A high degree of dilution is needed to prevent the formation of longer oligomers due to a further condensation of the formed products with additional equivalents of aldehyde. A ratio of 1 equivalent aldehyde to 25 – 30 equivalents pyrrole was found to be the optimal compromise for the prevention of side products using the smallest possible amount of pyrrole. Using trifluoroacetic acid (TFA) as a catalyst and commercially available pyrrole, 5-phenyldipyrromethane could easily be prepared in large amounts of high purity with a yield of 70%.^[1]



Scheme S1: Synthesis of the ancillary ligand precursor **5-phenyldipyrromethane**.

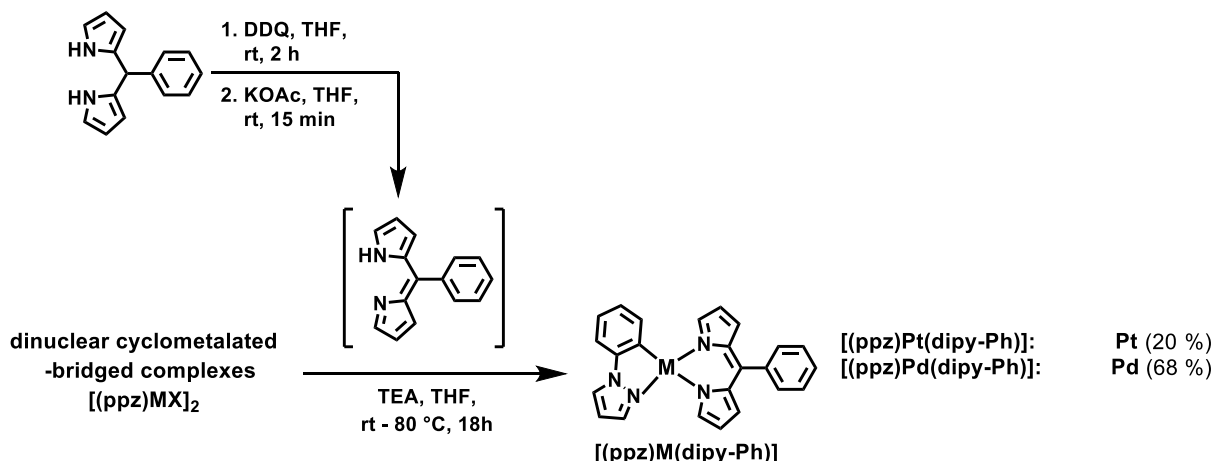
In the first step of the complex-synthesis commercially available **ppz** was treated with the respective transition metal source to form binuclear complexes as shown in **Scheme S2**.



Scheme S2: Synthesis of cyclometalated μ -bridged binuclear transition metal complexes of $[(ppz)MX]_2$.

The second step of the complex-synthesis is shown in **Scheme S3**. First, **5-phenyldipyrromethane** was oxidized to the ancillary ligand **dipy-Ph** with 2,3-dichloro-5,6-dicyano-1,4-benzoquinone (DDQ). After complete consumption of the starting material, potassium carbonate was added in order to deactivate any remaining DDQ and to increase the pH of the mixture. Without any work up, the binuclear complex was added and the reaction was stirred over night at rt for the Pt(II) and Pd(II) complexes.

All complexes were purified by flash column chromatography on silica. For the Pd(II)-compounds the silica gel had to be deactivated with 10 % TEA prior to use.



Scheme S3: Synthesis of the complexes [(ppz)Pt(dipy-Ph)] and [(ppz)Pd(dipy-Ph)] from the precursor of the ancillary ligand 5-phenyldipyromethane and the binuclear complexes [(ppz)PtCl₂]₂ and [(ppz)PdOAc]₂.

Experimental

All reactions were carried out under an atmosphere of nitrogen (dried with Sicapent from Merck, oxygen was removed with a cupric oxide catalyst R3-11 from BASF) using standard Schlenk-techniques.^[2] Solvent for oxygen and/or moisture sensitive reactions were freshly distilled under nitrogen from the appropriate dehydrating agent (sodium/benzophenone “ketyl blue” for THF, CaH₂ for CH₂Cl₂) and degassed with dry nitrogen before use. Solvents for chromatography and work-up procedures were of technical grade and distilled prior to use. Flash chromatography^[3] was performed on silica gel (Macherey-Nagel “Silica 60 M”, 40–63 μm) wet-packed in glass columns.

¹H and ¹³C NMR spectra were measured in deuterated solvents as indicated (acetone-*d*₆ and dichloromethane-*d*₂ (CD₂Cl₂)). Samples were filtered and placed in frequency-matched 5 mm glass sample tubes. Chemical shifts are given in ppm relative to the respective residual nondeuterated solvent signal (in ppm: ¹H: acetone: δ 2.05, CH₂Cl₂: 5.32,; ¹³C: CH₂Cl₂: 53.84).^[4] Deuterated solvents were used as received.

The abbreviations used to assign the spin multiplicities are: s = singlet, bs = broad singlet, d = doublet, dd = doublet of doublet, ddd = doublet of doublet of doublet, m = multiplet. Multiplet signals or overlapping signals in proton NMR spectra that could not be assigned to first order couplings are given as (-). The order of declaration for proton spectra is: chemical shift (spin multiplicity, coupling constant, number of protons). C-atom types are abbreviated as: CH = tertiary, C = quaternary.

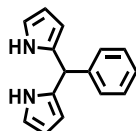
- Bruker Avance III HD 400 FT-Spectrometer (¹H: 400.13 MHz, ¹³C: 100.61 MHz) with a Bruker Ultrashield magnet
- Bruker Avance III HD 400 FT-Spectrometer (¹H: 400.03 MHz, ¹³C: 100.59 MHz) with a Bruker Ascend magnet
- Bruker Avance III HD 600 FT-Spectrometer (¹H: 600.13 MHz, ¹³C: 150.90 MHz) with an Oxford Instruments magnet (with cryoprobe unit, CPDCH 13C)
- Bruker Avance III HD 600 FT-Spectrometer (¹H: 600.43 MHz, ¹³C: 150.98 MHz) with a Bruker Ascend magnet

Mass spectra were recorded with a Bruker Daltonics autoflex II (MALDI) in positive mode (POS) using a DCTB (trans-2-[3-(4-tert-butylphenyl)-2-methyl-2-propenyl-iden]malononitrile) matrix or with a Bruker Daltonic microTOF focus (ESI). All mass spectrometry peaks are reported as m/z. For calculation of the respective mass

values of the isotopic distribution, the software module "Bruker Daltonics IsotopePattern" from the software Compass 1.1 from Bruker Daltonics GmbH, Bremen was used. Calculated (calc.) and measured (found) peak values correspond to the most intense peak of the isotopic distribution.

Elemental analyses were performed with a vario MICRO cube CHNS instrument at the Institut für Anorganische Chemie, Universität Würzburg.

5-Phenyldipyrromethane



CA: [107798-98-1]

Benzaldehyde (2.62 g, 2.50 ml, 24.7 mmol) and 1*H*-pyrrole (filtered over a small plug of alumina act. I directly prior to use) (41.5 g, 42.9 ml, 618 mmol) were added to a dry round-bottom Schlenk-flask and degassed with a stream of nitrogen for 15 min. TFA (282 mg, 190 μ l, 2.47 mmol) was added under nitrogen and the reaction mixture was stirred at rt for 10 min before it was quenched with TEA (10 ml). The reaction mixture was then distilled under reduced pressure at low temperature to yield a yellow to brown oil. The crude product was purified by flash column chromatography on silica (eluent: PE/DCM/EA = 8/1/1).^[1]

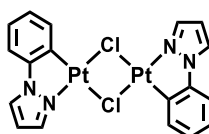
Yield: 3.82 mg (17.2 mmol, 70 %) of a greyish solid.

C₁₅H₁₄N₂ [222.29]

¹H-NMR (400 MHz, acetone-*d*₆):

δ [ppm] = 9.68 (bs, 2H), 7.30–7.15 (-, 5H), 6.67 (ddd, ³J_{HH} = 4.3 Hz, ³J_{HH} = 2.7 Hz, ⁴J_{HH} = 1.6 Hz, 2H), 5.97 (dd, ³J_{HH} = 3.1 Hz, ³J_{HH} = 2.7 Hz, ⁴J_{HH} = 2.7 Hz, 2H), 5.95-5.91 (m, 2H), 5.48 (s, 1H).

[(ppz)PtCl]₂



CA: [59161-16-9]

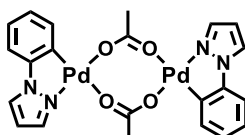
Synthesis according to lit.^[5,6]

Under nitrogen, K₂PtCl₄ (1.00 g, 2.41 mmol) and 1-phenylpyrazole (350 mg, 320 μ l, 2.41 mmol) were added to a degassed mixture of 2-ethoxyethanol and deionized water (30 ml, 3/1 by volume). The reaction mixture was stirred at 80 °C for 18 h. After the suspension cooled down to rt, distilled water (40 ml) was added and the precipitate was filtered off with a sintered glass funnel (P4) and washed with water (3 x 10 ml). The crude product was then dried under reduced pressure and was used without further purification.

Yield: 620 g (830 μ mol, 69 %) of a slightly grey solid.

C₁₈H₁₄Cl₂N₄Pt₂ [747.41]

[(ppz)PdOAc]₂



CA: [1263103-50-9]

Synthesis according to lit.^[7]

Under nitrogen, Pd(OAc)₂ (500 mg, 2.23 mmol) was added to a degassed solution of 1-phenylpyrazole (320 mg, 290 μl, 2.22 mmol) in dry DCM (20 ml). After stirring for at rt for 3h, the orange solution was concentrated nearly to dryness under reduced pressure and the residue is triturated with Et₂O (30 ml). The precipitate was then filtered off with a sintered glass funnel (P4) and washed with Et₂O (3 x 10 ml). The crude product was then dried under reduced pressure and was used without further purification.

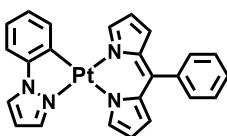
Yield: 640 mg (1.04 mmol, 94 %) of a yellow solid.

C₂₂H₂₀N₄O₄Pd₂ [617.25]

General procedure for the synthesis of cyclometalated dipyrinato-metal complexes [(ppz)M(dipy-Ph)] according to literature^[8, 9]

Under nitrogen the appropriate dipyrromethane (1.0 eq) was dissolved in dry THF and DDQ (1.1 eq) was added before the mixture was stirred at rt for 2 h. Then, finely powdered K₂CO₃ (10 eq) was added and the mixture was stirred for 15 min before the appropriate binuclear cyclometalated μ-bridged metal-dimer (0.5 eq) and TEA (2 ml) were added. The reaction was then stirred at rt or 80 °C for 18 h and cooled down to rt before DCM (20 ml) and celite (aprox. 10 g) were added. The resulting mixture was filtered through a small plug of celite which was rinsed with DCM until the eluent was colorless. The solvents were removed under reduced pressure and the crude product was purified by flash column chromatography on silica and if necessary with preparative recycling GPC (THF, 4 ml/min). Finally, the product was precipitated from DCM into MeOH. The obtained solid was again precipitated from DCM into n-pentane. The obtained desired compounds were analytically pure after drying under high vacuum (approx., 10⁻⁵ mbar) for 24 h.

[(ppz)Pt(dipy-Ph)]



CA: [-]

Synthesis following GP:

5-phenyldipyrromethane (89.0 mg, 402 μmol), DDQ (100 mg, 442 μmol), potassium carbonate (560 mg, 4.02 mmol), [(ppz)PtCl]₂ (150 mg, 201 μmol) in THF (10 ml), rt, 18 h; flash column chromatography (eluent: DCM/PE = 1/3 → 1/1).

Yield: 45.0 mg (80.0 μmol, 20 %) of a red solid.

C₂₄H₁₈N₄Pt [557.52]

¹H-NMR (400 MHz, CD₂Cl₂):

δ [ppm]= 8.12-8.11 (m, 1H), 8.10 (dd, $^3J_{H,H} = 2.9$ Hz, $^4J_{H,H} = 0.6$ Hz, 1H), 8.03-8.02 (m, 1H), 7.92 (d, $^3J_{H,H} = 2.4$ Hz, 1H), 7.53-7.44 (-, 5H), 7.35-7.33 (m, 1H), 7.29-7.27 (m, 1H), 7.18-7.10 (-, 2H), 6.86 (dd, $^3J_{H,H} = 4.3$ Hz, $^3J_{H,H} = 1.2$ Hz, 1H), 6.63-6.61 (-, 2H), 6.57 (dd, $^3J_{H,H} = 4.3$ Hz, $^4J_{H,H} = 1.5$ Hz, 1H), 6.47 (dd, $^3J_{H,H} = 4.4$ Hz, $^3J_{H,H} = 1.7$ Hz, 1H).

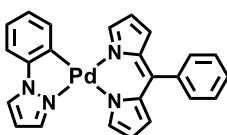
$^{13}\text{C-NMR}$ (100 MHz, CD_2Cl_2):

δ [ppm] = 152.3 (CH), 150.9 (CH), 148.5 (C), 145.4 (C), 140.2 (CH), 138.1 (C), 137.3 (C), 136.4 (C), 135.7 (CH), 131.8 (CH), 131.4 (CH), 131.3 (C), 130.9 (CH), 128.9 (CH), 127.7 (CH), 126.9 (CH), 125.6 (CH), 124.2 (CH), 117.5 (CH), 117.1 (CH), 111.0 (CH), 107.3 (CH).

Microanalysis (CHN): calc. for $\text{C}_{24}\text{H}_{18}\text{N}_4\text{Pt}$ C-%: 51.70, H-%: 3.25, N-%: 10.05
found for $\text{C}_{24}\text{H}_{18}\text{N}_4\text{Pt}$ C-%: 51.67, H-%: 3.45, N-%: 10.07.

ESI-MS (pos., high res.): $[\text{M}^{+}] = \text{C}_{24}\text{H}_{18}\text{N}_4\text{Pt}$; calc.: 557.11757, found: 557.11712
 $\Delta = 0.81$ ppm

[(ppz)Pd(dipy-Ph)]



CA: [-]

Synthesis following GP:

5-phenyldipyrromethane (58.0 mg, 261 μmol), DDQ (65.0 mg, 286 μmol), potassium carbonate (360 mg, 2.60 mmol), [(ppz)PdOAc]₂ (80.0 mg, 130 μmol) in THF (10 ml), rt, 18 h; flash column chromatography (eluent: $\text{Et}_2\text{O}/\text{PE}/\text{TEA} = 30/20/1$).

Yield: 83.0 mg (177 μmol , 68 %) of a orange solid.

$\text{C}_{24}\text{H}_{18}\text{N}_4\text{Pd}$ [468.84]

$^1\text{H-NMR}$ (400 MHz, CD_2Cl_2):

δ [ppm]= 8.10 (dd, $^3J_{H,H} = 2.8$ Hz, $^4J_{H,H} = 0.6$ Hz, 1H), 7.98-7.95 (-, 2H), 7.85 (dd, $^3J_{H,H} = 1.3$, $^3J_{H,H} = 1.3$ Hz, 1H), 7.53-7.42 (-, 5H), 7.32-7.29 (m, 1H), 7.23 (dd, $^3J_{H,H} = 7.8$ Hz, $^4J_{H,H} = 1.5$ Hz, 1H), 7.20-7.15 (m, 1H), 7.08 (ddd, $^3J_{H,H} = 7.6$ Hz, $^3J_{H,H} = 7.1$ Hz, $^4J_{H,H} = 1.5$ Hz, 1H), 6.78 (dd, $^3J_{H,H} = 4.3$ Hz, $^4J_{H,H} = 1.2$ Hz, 1H), 6.59 (dd, $^3J_{H,H} = 2.7$ Hz, $^3J_{H,H} = 2.4$ Hz, 1H), 6.55 (dd, $^3J_{H,H} = 2.4$ Hz, $^4J_{H,H} = 1.4$ Hz, 1H), 6.51 (dd, $^3J_{H,H} = 4.3$ Hz, $^4J_{H,H} = 1.4$ Hz, 1H), 6.46 (dd, $^3J_{H,H} = 4.3$ Hz, $^4J_{H,H} = 1.6$ Hz, 1H).

$^{13}\text{C-NMR}$ (100 MHz, CD_2Cl_2):

δ [ppm] = 152.6 (CH), 151.2 (CH), 148.5 (C), 144.6 (C), 141.0 (CH), 140.6 (C), 138.9 (C), 138.5 (C), 137.9 (C), 137.2 (CH), 132.1 (CH), 131.6 (CH), 131.1 (CH), 128.9 (CH), 127.6 (CH), 126.2 (CH), 125.7 (CH), 125.2 (CH), 117.8 (CH), 117.3 (CH), 111.5 (CH), 107.4 (CH).

Microanalysis (CHN): calc. for $\text{C}_{24}\text{H}_{18}\text{N}_4\text{Pd}$ C-%: 61.48, H-%: 3.87, N-%: 11.95
found for $\text{C}_{24}\text{H}_{18}\text{N}_4\text{Pd}$ C-%: 61.71, H-%: 3.65, N-%: 11.81.

ESI-MS (pos., high res.): $[\text{M}^{+}] = \text{C}_{24}\text{H}_{18}\text{N}_4\text{Pd}$; calc.: 468.05701, found: 468.05671
 $\Delta = 0.64$ ppm

Steady-State Absorption Spectroscopy

- JASCO V-670 UV/Vis/NIR spectrometer (software SpectraManager v. 2.08.04)
- Agilent Technologies Cary 5000 UV-Vis-NIR spectrophotometer (software Agilent Cary WinUV Analysis and Bio v.4.2)

The solvent THF was distilled prior to use. Absorption spectra were recorded in 1 cm quartz cuvettes from Starna (Pfungstadt, Germany) at rt. Aggregation of the samples could be excluded by a concentration independent behaviour (10^{-6} – 10^{-5} M).

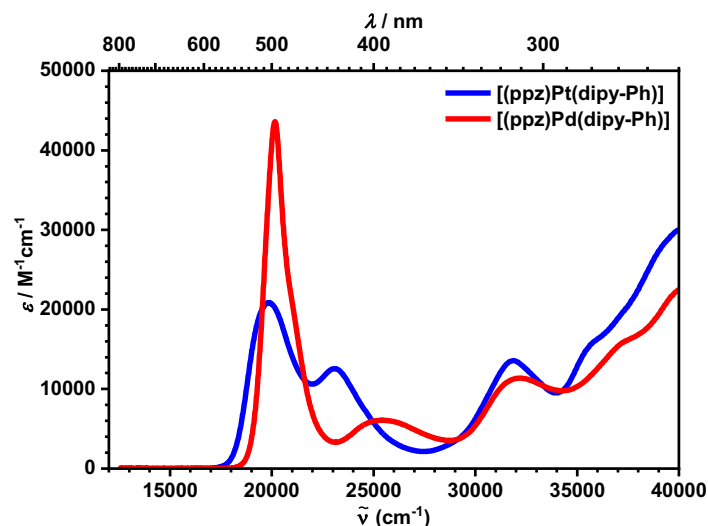


Figure S1: Absorption spectra of, **[(ppz)Pt(dipy-Ph)]** (blue) and **[(ppz)Pd(dipy-Ph)]** (red) in THF at rt.

Steady-State Emission Spectroscopy

- Edinburgh Instruments FLS980 fluorescence lifetime spectrometer including a 450 W xenon lamp (software F980 version 1.2.2)
- single photon counting photomultiplier (R928P), working range 200-850 nm

Steady state emission spectra at room temperature were recorded in 1 cm quartz cells from Starna (Pfungstadt, Germany). 2-MeTHF was of spectroscopic grade and was used without further purification, THF was distilled prior to use. The concentration was ca. 10^{-6} – 10^{-5} M and oxygen was removed by sparging with Argon for at least 30 min before each measurement.

Emission spectra at 77 K in a 2-MeTHF glassy matrix were measured in EPR quartz tubes (5 mm diameter) and were cooled to 77 K in an EPR *Dewar* vessel with liquid nitrogen.

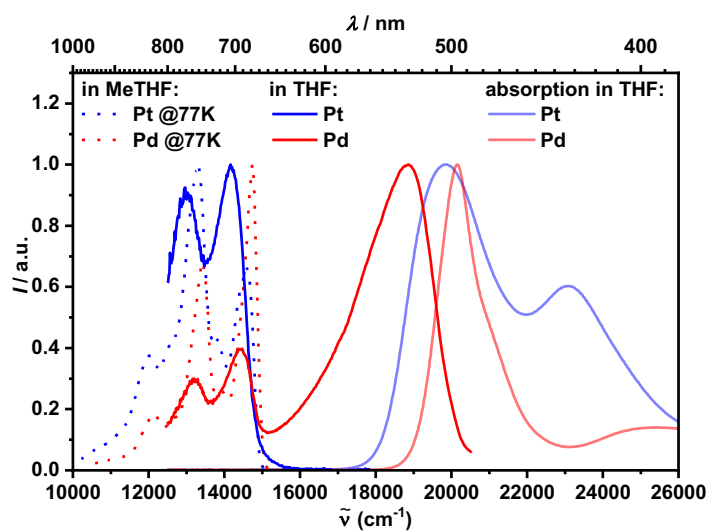


Figure S2: Normalized emission spectra at 77 K in 2-MeTHF (dotted lines) and at rt in THF (solid lines) of **[(ppz)Pt(dipy-Ph)]** (blue) and **[(ppz)Pd(dipy-Ph)]** (red) in comparison with the respective normalized steady state absorption spectra at rt in THF (pale lines).

Table S1: Selected geometrical parameters of the X-ray structure by Hanson *et al.*^[8] and the optimized S0 iridium structure. The optimized S0 structure is an enantiomer of the crystal structure.

	X-ray	S0
	Distances [Å]	
Ir1 C12	2.02	2.03
Ir1 N22	2.02	2.04
Ir1 N38	2.11	2.16
Ir1 N39	2.12	2.16
N38 C53	1.34	1.33
C53 C51	1.42	1.42
C51 C49	1.37	1.38
C49 C40	1.43	1.43
C40 N38	1.41	1.39
C40 C42	1.39	1.41
C42 C41	1.41	1.41
N39 C47	1.34	1.33
C47 C45	1.41	1.42
C45 C43	1.38	1.38
C43 C41	1.42	1.43
C41 N39	1.39	1.39
	Angles [°]	
C12 Ir1 N22	80.2	79.5
N38 Ir1 N39	86.7	86.6
N12 Ir1 N38	91.4	92.8
N39 Ir1 C2	92.6	93.0
C2 Ir1 C12	89.9	88.1
	Torsion angles [°]	
C2 C12 N38 N39	8.7	-8.4
C41 C42 C55 C58	-113.6	107.5
C16 C15 N24 C27	-1.2	-0.2
C43 C41 C42 C55	-8.5	-0.6
C49 C40 C42 C55	12.4	-0.7
Ir1 N38 N39 C41	-163.8	-179.3
Ir1 N39 N38 C40	164.6	179.1

Table S2: Selected geometrical parameters of the optimized iridium structures.

	S0	TLC	SLC	SMLCT/LC	TMC
Distances [Å]					
Ir1 C12	2.03	2.03	2.03	2.04	2.04
Ir1 C2	2.03	2.03	2.03	2.04	2.05
Ir1 N22	2.04	2.04	2.04	2.06	2.59
Ir1 N23	2.04	2.04	2.04	2.06	2.33
Ir1 N38	2.16	2.16	2.16	2.14	2.15
Ir1 N39	2.16	2.16	2.16	2.08	2.11
N38 C53	1.33	1.37	1.34	1.36	1.33
C53 C51	1.42	1.41	1.42	1.40	1.42
C51 C49	1.38	1.38	1.38	1.40	1.38
C49 C40	1.43	1.47	1.45	1.42	1.43
C40 N38	1.39	1.35	1.38	1.38	1.39
C40 C42	1.41	1.42	1.44	1.42	1.40
C42 C41	1.41	1.42	1.44	1.38	1.41
N39 C47	1.33	1.37	1.35	1.38	1.34
C47 C45	1.42	1.41	1.42	1.43	1.41
C45 C43	1.38	1.38	1.38	1.40	1.39
C43 C41	1.43	1.47	1.45	1.38	1.42
C41 N39	1.39	1.35	1.38	1.45	1.39
Angles [°]					
C12 Ir1 N22	79.5	79.5	79.5	78.3	71.6
C2 Ir1 N23	79.5	79.5	79.5	78.3	75.8
N38 Ir1 N39	86.6	85.9	85.3	87.9	88.2
N12 Ir1 N38	92.8	93.3	94.0	96.3	81.7
N39 Ir1 C2	93.0	93.4	93.9	92.0	95.3
C2 Ir1 C12	88.1	87.9	87.5	84.9	86.9
Torsion angles [°]					
C2 C12 N38 N39	-8.4	-8.4	-8.4	-12.0	-19.0
C41 C42 C55 C58	107.5	108.0	126.3	128.0	-69.6
C16 C15 N24 C27	-0.2	0.1	-0.4	-1.4	-16.4
C43 C41 C42 C55	-0.6	-1.1	-5.7	-16.9	-4.0
C49 C40 C42 C55	-0.7	-0.9	-3.7	-1.3	-0.1
Ir1 N38 N39 C41	-179.3	-179.1	178.3	-167.2	-175.2
Ir1 N39 N38 C40	179.1	179.2	176.9	159.6	174.5

Table S3: Selected geometrical parameters of the twist conformer of the platinum complex.

	S0	S(ML+LL)CT/LC	TLC	TMC
Distances [Å]				
Pt1 C19	2.01	2.01	2.01	2.11
Pt1 N22	2.06	2.07	2.06	2.15
Pt1 N2	2.13	2.04	2.12	2.14
Pt1 N12	2.02	2.01	2.02	2.06
N12 C8	1.39	1.39	1.35	1.39
C8 C9	1.43	1.42	1.46	1.43
C9 C10	1.38	1.40	1.38	1.38
C10 C11	1.41	1.39	1.40	1.41
C11 N12	1.34	1.36	1.38	1.34
C8 C7	1.40	1.41	1.42	1.41
C7 C6	1.40	1.45	1.42	1.41
C6 C5	1.43	1.40	1.47	1.43
C5 C4	1.38	1.43	1.38	1.38
C4 C3	1.41	1.37	1.41	1.41
C3 N2	1.33	1.39	1.38	1.33
N2 C6	1.39	1.38	1.35	1.39
Angles [°]				
C19 Pt1 N22	79.3	79.6	79.3	77.0
N22 Pt1 N2	99.4	98.4	99.7	98.2
N2 Pt1 N12	87.9	89.8	87.5	88.8
N12 Pt1 C19	96.9	97.3	97.1	111.5
Torsion angles [°]				
C19 N22 N2 N12	20.8	27.9	20.8	-59.8
C8 C7 C13 C14	118.1	127.6	122.6	115.5
C26 C20 N21 C25	-14.7	-11.5	-14.9	-4.3
C9 C8 C7 C13	-13.9	-8.4	-12.9	-5.1
C13 C7 C6 C5	-6.3	-7.1	-6.5	-5.0
C23 N22 N2 C3	35.1	41.7	36.9	-47.9
Pt1 N2 N12 C8	-172.9	-177.6	-176.9	174.8
Pt1 N12 N2 C6	167.3	170.2	168.7	179.9

Table S4: Selected geometrical parameters of the butterfly conformer of the platinum complex.

	S0	S(ML+LL)CT/LC	SLC	TLC
Distances [Å]				
Pt1 C19	2.02	2.01	2.04	2.02
Pt1 N22	2.05	2.08	2.06	2.04
Pt1 N2	2.12	2.03	2.10	2.12
Pt1 N12	2.02	2.02	2.03	2.02
N12 C8	1.39	1.39	1.41	1.36
C8 C9	1.43	1.42	1.42	1.46
C9 C10	1.38	1.40	1.38	1.38
C10 C11	1.41	1.39	1.41	1.41
C11 N12	1.33	1.36	1.33	1.37
C8 C7	1.41	1.42	1.42	1.42
C7 C6	1.41	1.46	1.43	1.42
C6 C5	1.43	1.39	1.42	1.46
C5 C4	1.38	1.43	1.38	1.38
C4 C3	1.42	1.37	1.42	1.41
C3 N2	1.33	1.38	1.33	1.37
N2 C6	1.39	1.38	1.39	1.36
Angles [°]				
C19 Pt1 N22	79.3	79.2	79.1	79.4
N22 Pt1 N2	98.3	97.7	98.4	98.9
N2 Pt1 N12	85.1	85.6	83.1	84.2
N12 Pt1 C19	97.4	97.4	99.5	97.6
Torsion angles [°]				
C19 N22 N2 N12	-4.2	-10.8	-2.3	-4.2
C8 C7 C13 C14	113.5	136.1	133.5	119.5
C26 C20 N21 C25	-2.4	-4.7	-2.7	-1.8
C9 C8 C7 C13	14.7	11.3	19.2	12.3
C13 C7 C6 C5	-13.1	-21.8	-23.5	-12.1
C23 N22 N2 C3	19.1	18.2	25.7	20.5
Pt1 N2 N12 C8	-146.9	-148.47	-145.1	-150.1
Pt1 N12 N2 C6	148.8	144.9	145.8	152.0

Table S5: Relative energies of the four conformers found for the palladium complex. The lowest energy has been set to 0 for both DFT and DFT/MRCI.

	DFT/MRCI	DFT
	ΔE [eV]	ΔE [eV]
Conformer 1	0.040	0.027
Conformer 2	0.007	0.006
Conformer 3	0	0.023
Conformer 4	0.034	0

Table S6: Selected geometrical parameters of conformer 1 of the palladium complex.

	S0	SILCT	TLC
Distances			
Pd1 C19	2.01	1.99	2.01
Pd1 N22	2.05	2.03	2.05
Pd1 N2	2.10	2.15	2.10
Pd1 N12	2.02	2.04	2.02
N12 C8	1.39	1.37	1.36
C8 C9	1.43	1.43	1.46
C9 C10	1.38	1.37	1.38
C10 C11	1.41	1.44	1.41
C11 N12	1.33	1.33	1.37
C8 C7	1.41	1.48	1.42
C7 C6	1.41	1.43	1.43
C6 C5	1.43	1.41	1.46
C5 C4	1.38	1.40	1.38
C4 C3	1.42	1.41	1.42
C3 N2	1.33	1.34	1.36
N2 C6	1.38	1.39	1.36
Angles			
C19 Pd1 N22	79.7	80.3	79.8
N22 Pd1 N2	98.0	98.1	98.9
N2 Pd1 N12	85.8	85.0	84.8
N12 Pd1 C19	96.6	96.7	96.7
Torsion angles			
C19 N22 N2 N12	-4.3	-1.1	-5.3
C6 C7 C13 C14	-72.2	-6.4	-68.8
C8 C7 C13 C14	113.6	173.4	173.4
C26 C20 N21 C25	-2.4	-3.7	-0.9
C9 C8 C7 C13	14.2	82.8	12.8
C13 C7 C6 C5	-12.6	-44.5	-13.8
C23 N22 N2 C3	18.2	22.7	18.8
Pd1 N2 N12 C8	-145.9	-133.9	-148.2
Pd1 N12 N2 C6	147.6	155.3	149.5

Table S7: Selected geometrical parameters of conformer 2 of the palladium complex.

	S0	SMLCT/LC	TLC	TMLCT/LC	TMC
Distances					
Pd1 C19	2.00	2.00	2.00	2.01	2.10
Pd1 N22	2.06	2.07	2.06	2.08	2.23
Pd1 N2	2.11	2.03	2.10	2.08	2.14
Pd1 N12	2.03	1.99	2.02	1.99	2.11
N12 C8	1.39	1.38	1.35	1.38	1.39
C8 C9	1.43	1.42	1.46	1.42	1.43
C9 C10	1.38	1.40	1.38	1.40	1.38
C10 C11	1.41	1.39	1.41	1.40	1.41
C11 N12	1.34	1.36	1.38	1.36	1.33
C8 C7	1.41	1.42	1.42	1.42	1.41
C7 C6	1.40	1.45	1.42	1.42	1.41
C6 C5	1.43	1.40	1.47	1.39	1.43
C5 C4	1.38	1.43	1.38	1.45	1.38
C4 C3	1.42	1.37	1.41	1.37	1.42
C3 N2	1.33	1.38	1.37	1.37	1.33
N2 C6	1.39	1.37	1.35	1.41	1.38
Angles					
C19 Pd1 N22	79.8	80.1	79.8	79.8	76.8
N22 Pd1 N2	99.2	99.0	99.5	99.8	101.1
N2 Pd1 N12	89.0	90.6	88.4	90.1	88.3
N12 Pd1 C19	96.5	96.9	96.5	96.2	117.6
Torsion angles					
C19 N22 N2 N12	22.6	32.1	22.3	27.9	-68.1
C6 C7 C13 C14	121.6	129.0	125.9	126.2	115.2
C8 C7 C13 C14	-59.7	-51.6	-56.5	-52.7	-64.7
C26 C20 N21 C25	-14.3	-9.7	-15.5	-13.9	0.2
C9 C8 C7 C13	-14.7	-7.3	-14.1	-11.8	-3.9
C13 C7 C6 C5	-6.4	-7.0	-6.2	-6.6	-4.5
C23 N22 N2 C3	36.7	44.2	38.4	43.5	-58.1
Pd1 N2 N12 C8	169.5	170.7	166.2	165.8	175.9
Pd1 N12 N2 C6	-173.0	-178.3	-176.0	-175.6	180.0

Table S8: Selected geometrical parameters of conformer 3 of the palladium complex.

	S0	SMLCT/LC	TLC
Distances			
Pd1 C19	2.00	2.00	2.01
Pd1 N22	2.08	2.09	2.05
Pd1 N2	2.13	2.03	2.11
Pd1 N12	2.01	1.99	2.01
N12 C8	1.38	1.38	1.35
C8 C9	1.43	1.42	1.46
C9 C10	1.38	1.40	1.38
C10 C11	1.41	1.40	1.41
C11 N12	1.33	1.35	1.37
C8 C7	1.41	1.42	1.43
C7 C6	1.40	1.46	1.42
C6 C5	1.43	1.38	1.46
C5 C4	1.38	1.45	1.38
C4 C3	1.42	1.37	1.42
C3 N2	1.33	1.38	1.36
N2 C6	1.39	1.39	1.36
Angles			
C19 Pd1 N22	79.5	79.6	79.8
N22 Pd1 N2	100.6	99.5	99.3
N2 Pd1 N12	86.6	86.2	84.5
N12 Pd1 C19	94.3	95.2	96.4
Torsion angles			
C19 N22 N2 N12	-10.8	-10.2	-4.0
C6 C7 C13 C14	-116.1	-137.6	-131.8
C8 C7 C13 C14	69.9	50.6	61.1
C26 C20 N21 C25	3.46	-2.8	-2.3
C9 C8 C7 C13	15.8	19.3	20.4
C13 C7 C6 C5	-2.6	-3.9	-7.4
C23 N22 N2 C3	-0.1	8.3	16.1
Pd1 N2 N12 C8	-149.3	-141.7	-145.0
Pd1 N12 N2 C6	155.1	148.3	151.1

Table S9: Selected geometrical parameters of conformer 4 of the palladium complex.

	S0	SILCT	TLC	TMLCT/LC
Distances				
Pd1 C19	2.01	1.99	2.01	2.03
Pd1 N22	2.06	2.03	2.05	2.05
Pd1 N2	2.12	2.15	2.11	2.09
Pd1 N12	2.01	2.04	2.01	1.96
N12 C8	1.39	1.37	1.35	1.40
C8 C9	1.43	1.43	1.46	1.39
C9 C10	1.38	1.37	1.38	1.47
C10 C11	1.41	1.44	1.42	1.36
C11 N12	1.33	1.33	1.37	1.39
C8 C7	1.41	1.48	1.43	1.43
C7 C6	1.41	1.43	1.42	1.42
C6 C5	1.43	1.41	1.46	1.42
C5 C4	1.38	1.40	1.38	1.40
C4 C3	1.42	1.41	1.41	1.40
C3 N2	1.33	1.34	1.36	1.35
N2 C6	1.39	1.39	1.36	1.38
Angles				
C19 Pd1 N22	79.7	80.3	79.8	79.5
N22 Pd1 N2	99.0	98.0	99.4	97.4
N2 Pd1 N12	85.7	85.0	84.5	85.7
N12 Pd1 C19	95.8	96.7	96.3	97.4
Torsion angles				
C19 N22 N2 N12	-5.9	-1.1	-4.1	-2.0
C6 C7 C13 C14	-122.8	-6.5	-132.0	-131.2
C8 C7 C13 C14	63.0	173.8	60.8	59.1
C26 C20 N21 C25	-1.1	-3.7	-2.4	-4.4
C9 C8 C7 C13	18.9	82.8	20.0	17.2
C13 C7 C6 C5	-6.0	-44.5	-7.1	-5.4
C23 N22 N2 C3	11.5	22.7	16.5	19.5
Pd1 N2 N12 C8	-143.4	-133.9	-145.5	-139.2
Pd1 N12 N2 C6	149.8	155.3	151.5	147.1

Table S10: Selected geometrical parameters for the X-ray structures of the platinum and palladium complexes.

	M = Pt, a	M = Pt, b	M = Pd
Distances			
M C19	2.02	2.03	2.00
M N22	2.02	2.02	2.03
M N2	2.09	2.07	2.10
M N12	2.01	2.03	2.01
N12 C8	1.41	1.40	1.38
C8 C9	1.42	1.44	1.42
C9 C10	1.39	1.35	1.38
C10 C11	1.40	1.41	1.41
C11 N12	1.34	1.32	1.35
C8 C7	1.39	1.39	1.41
C7 C6	1.42	1.39	1.39
C6 C5	1.43	1.43	1.44
C5 C4	1.38	1.39	1.37
C4 C3	1.43	1.40	1.42
C3 N2	1.33	1.33	1.33
N2 C6	1.40	1.39	1.40
Angles			
C19 M N22	79.9	80.6	80.3
N22 M N2	97.7	95.2	98.6
N2 M N12	85.7	86.3	85.8
N12 M C19	96.8	97.9	95.5
Torsion angles			
C19 N22 N2 N12	3.6	-2.7	-6.4
C6 C7 C13 C14	-59.3	-115.6	-119.1
C8 C7 C13 C14	115.0	57.7	66.3
C26 C20 N21 C25	3.7	10.5	-2.9
C9 C8 C7 C13	-20.4	-9.2	22.7
C13 C7 C6 C5	10.8	13.9	-13.6
C23 N22 N2 C3	-18.8	-32.7	13.9
M N2 N12 C8	-152.8	-151.8	-143.7
M N12 N2 C6	148.2	155.5	149.2

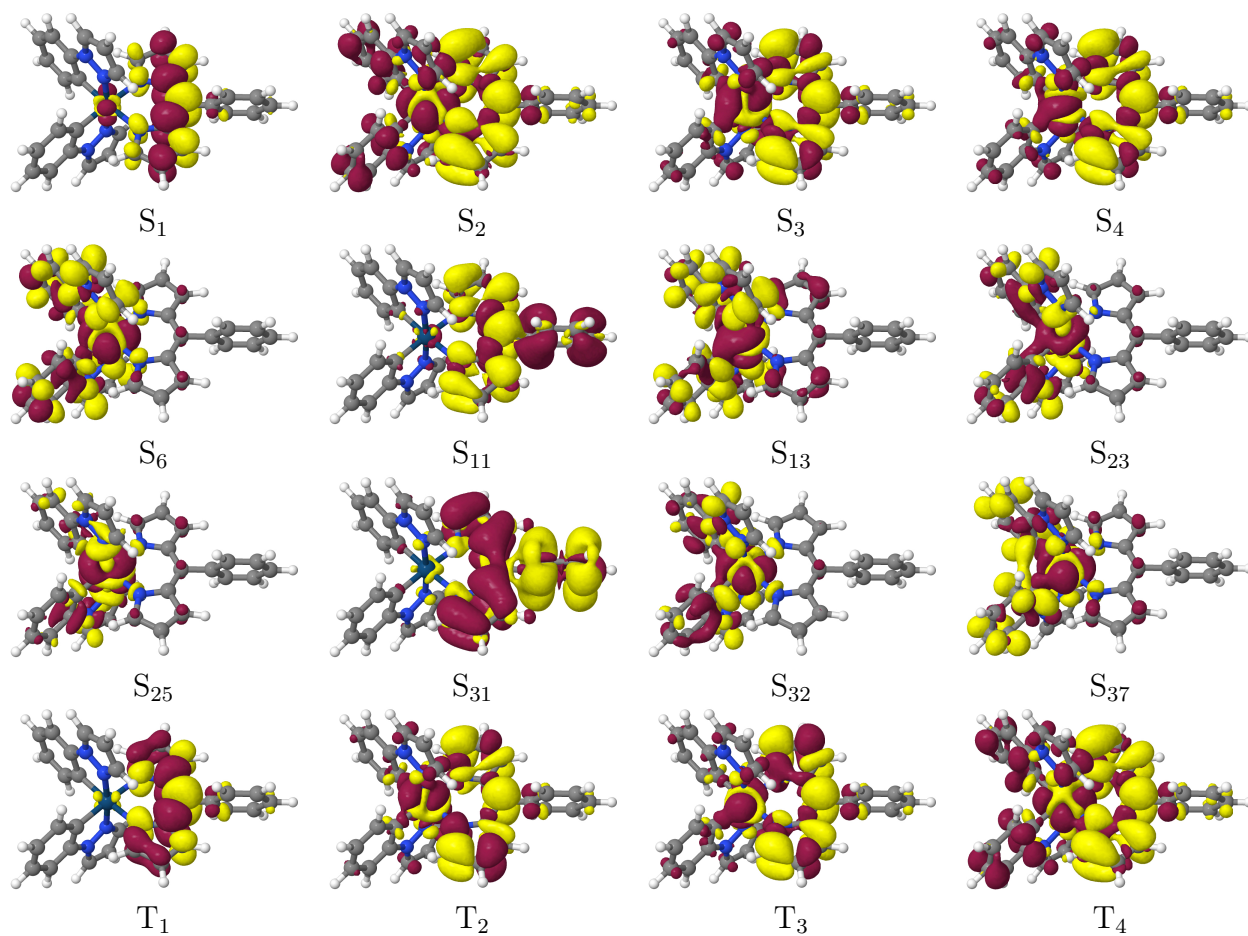


Figure S3: DFT/MRCI difference densities of the Ir complex at the S_0 geometry. Areas losing electron density upon electronic excitation from the ground state are shown in red, areas gaining electron density in yellow.

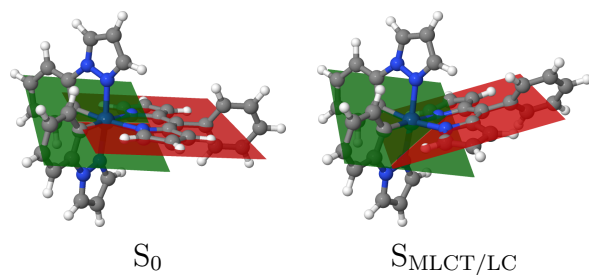


Figure S4: Coordination geometries of the Ir complex in the electronic ground state (a) and in the $S_{MLCT/LC}$ (b) state. The green plane is defined by the Ir atom and the C2 and C12 atoms of the ppz ligand, the red plane by the N38, N39 and C42 atoms of the dipy ligand. The planes show a small twist angle at the S_0 minimum, while the dipy ligand is bent out of the coordination plane at the $S_{MLCT/LC}$ minimum. For the atom labeling, see Fig. 1.

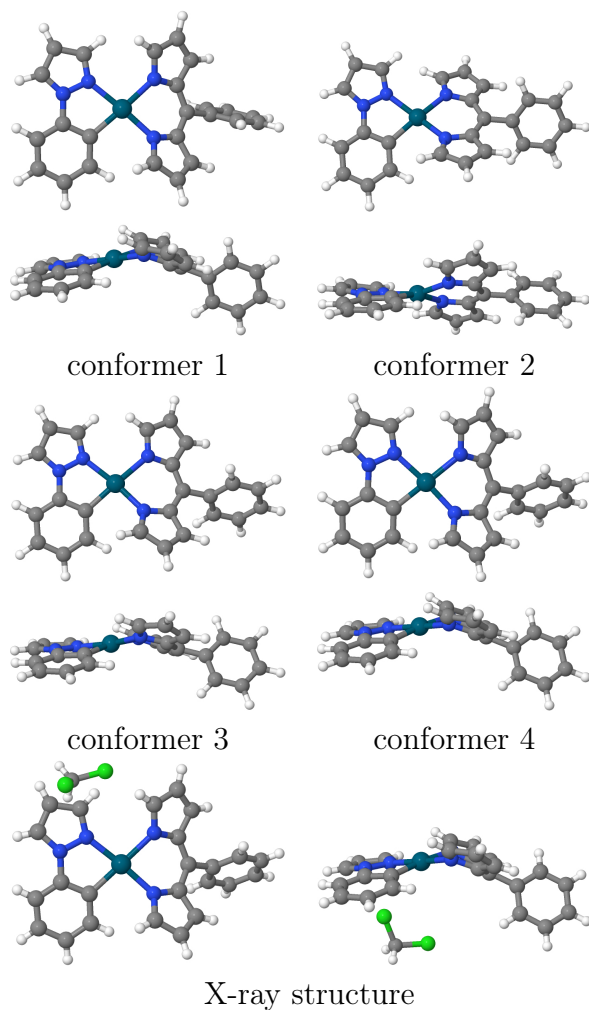


Figure S5: Perspective views of the four different ground state structures of the palladium complex compared to the X-ray structure which contains a co-crystallized dichloromethane solvent molecule as well.

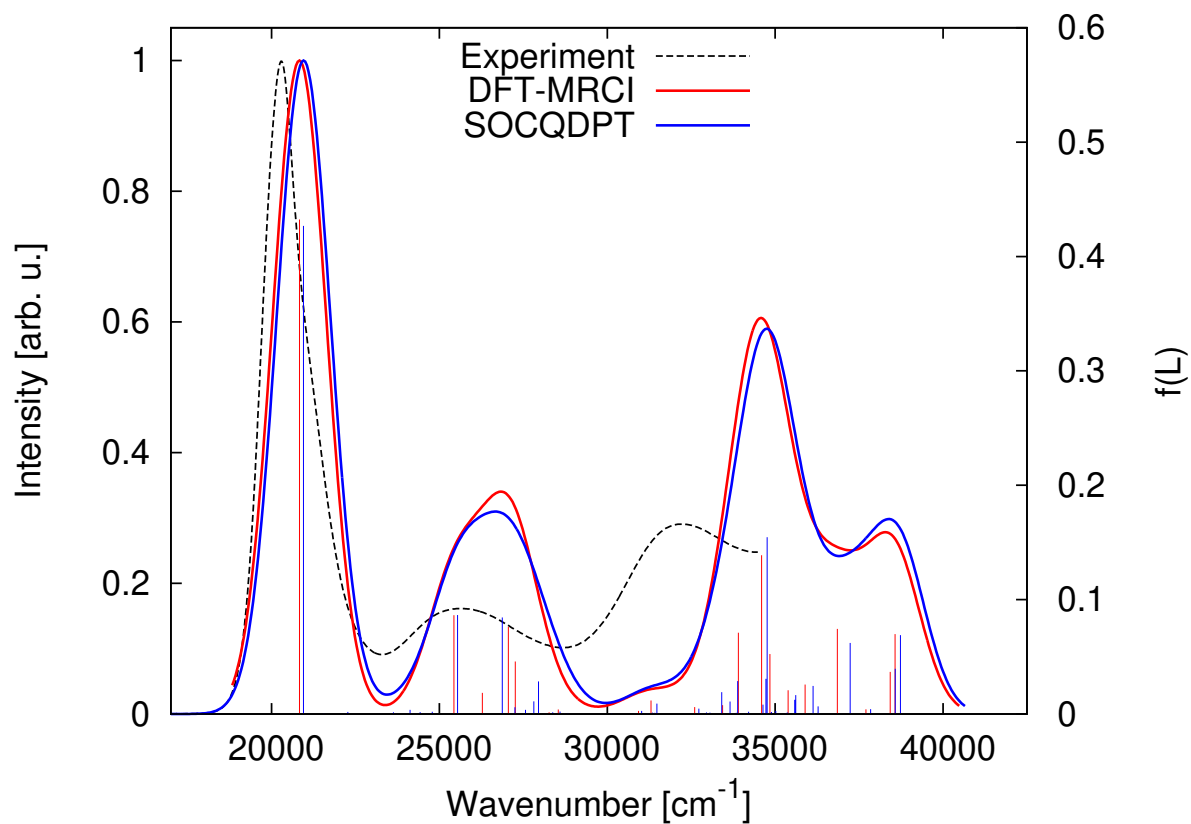


Figure S6: Spin-orbit coupled absorption spectrum of conformer 1 of the Pd-complex in comparison with the spin-free and the experimental spectrum. The calculated line spectra (oscillator strength $f(L)$, right y-axis) were broadened with Gaussians of 800 cm^{-1} full width at half maximum. The maximum intensity of the highest peak of the theoretical spectrum has been normalized to one (intensity on the left y-axis).

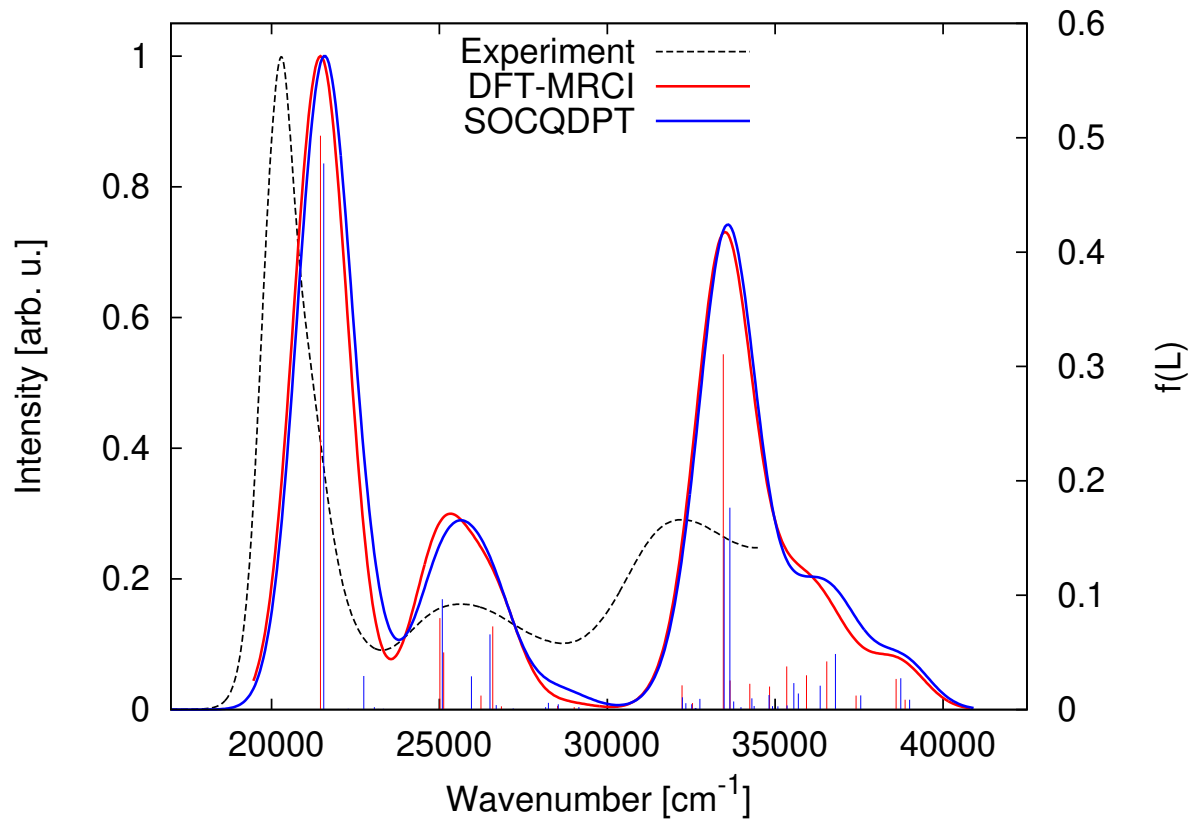


Figure S7: Spin-orbit coupled absorption spectrum of conformer 2 of the Pd-complex in comparison with the spin-free and the experimental spectrum. The calculated line spectra (oscillator strength $f(L)$, right y-axis) were broadened with Gaussians of 800 cm^{-1} full width at half maximum. The maximum intensity of the highest peak of the theoretical spectrum has been normalized to one (intensity on the left y-axis).

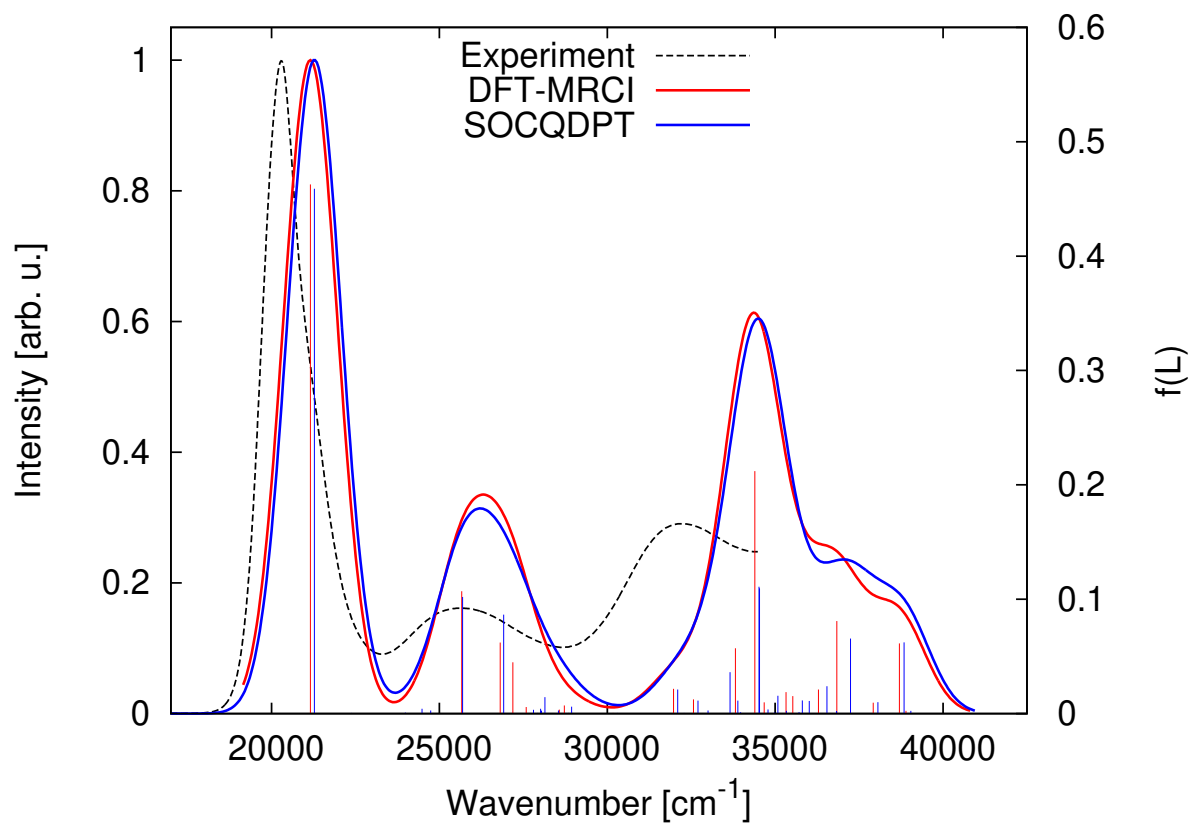


Figure S8: Spin-orbit coupled absorption spectrum of conformer 3 of the Pd-complex in comparison with the spin-free and the experimental spectrum. The calculated line spectra (oscillator strength $f(L)$, right y-axis) were broadened with Gaussians of 800 cm^{-1} full width at half maximum. The maximum intensity of the highest peak of the theoretical spectrum has been normalized to one (intensity on the left y-axis).

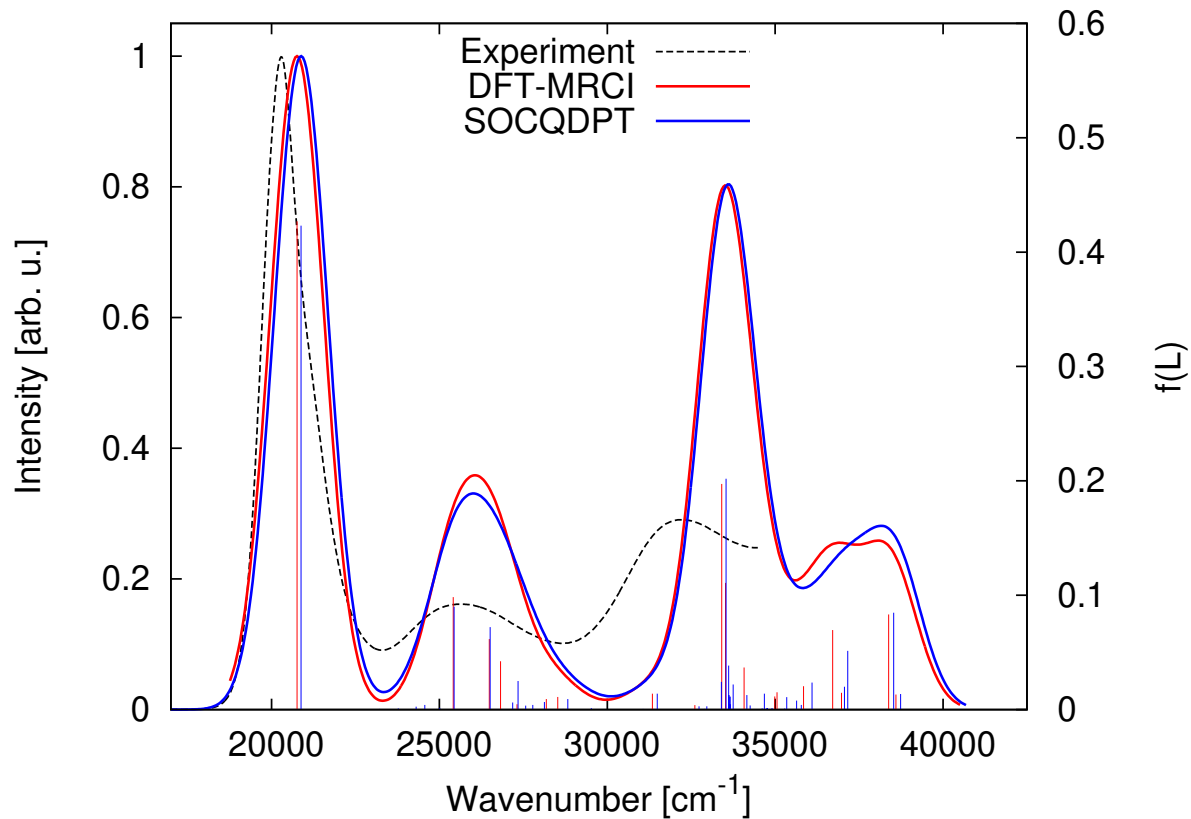


Figure S9: Spin-orbit coupled absorption spectrum of conformer 4 of the Pd-complex in comparison with the spin-free and the experimental spectrum. The calculated line spectra (oscillator strength $f(L)$, right y-axis) were broadened with Gaussians of 800 cm^{-1} full width at half maximum. The maximum intensity of the highest peak of the theoretical spectrum has been normalized to one (intensity on the left y-axis).

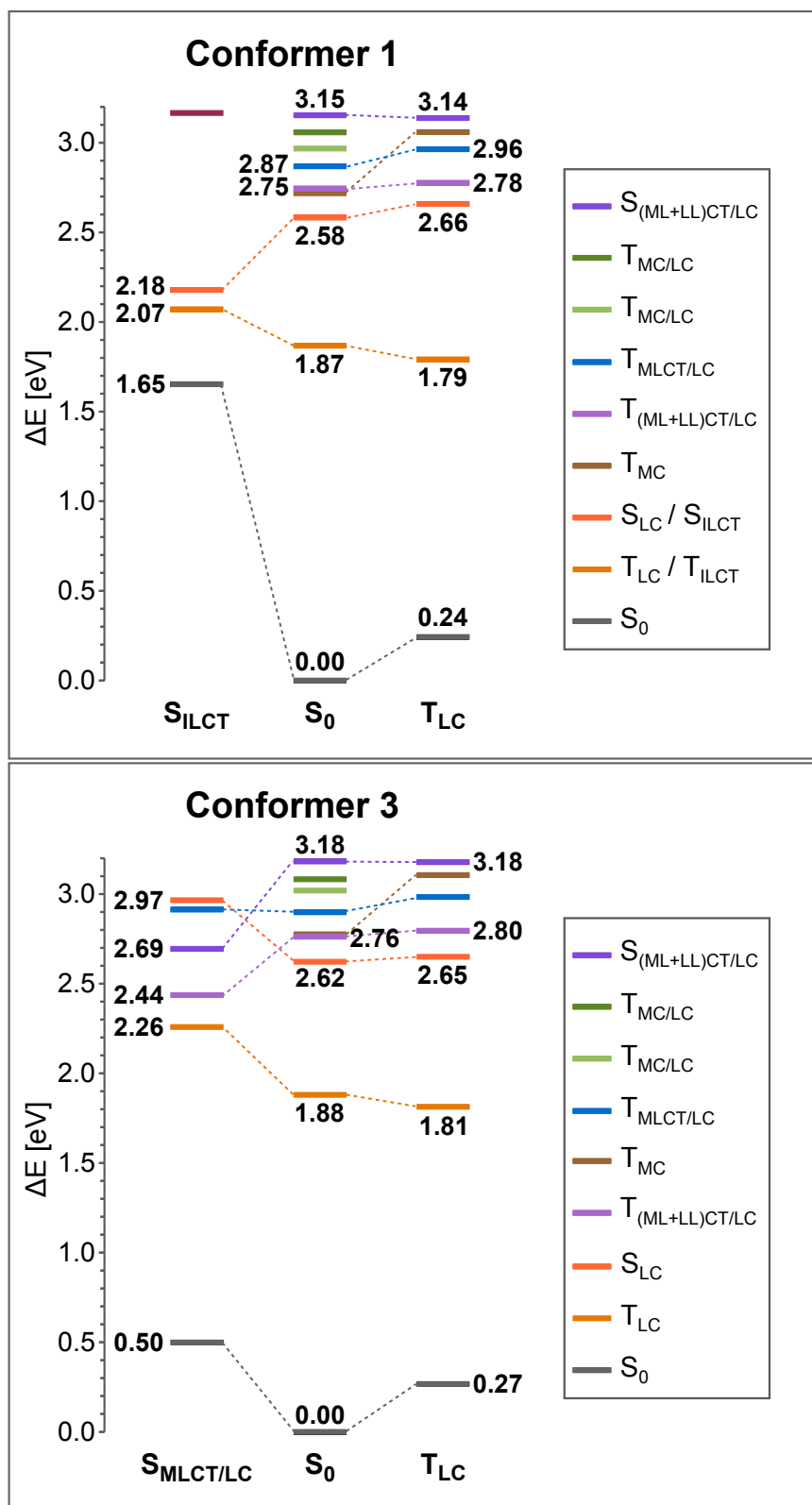


Figure S10: DFT/MRCI energy profiles of the lowest excited singlet and triplet states of conformer 1 (top) and 3 (bottom) conformers of the Pd complex. All energies are given relative to the respective S_0 energy of that conformer.

References

- [1] B. J. Littler, M. A. Miller, C. H. Hung, R. W. Wagner, D. F. O'Shea, P. D. Boyle, J. S. Lindsey, *J. Org. Chem.* **1999**, *64*, 1391-1396.
- [2] D. F. Shriver, Drezdon M. A., *The manipulation of air-sensitive compounds*, John Wiley & Sons, New York, **1986**.
- [3] W. C. Still, M. Kahn, A. Mitra, *J. Org. Chem.* **1978**, *43*, 2923-2925.
- [4] G. R. Fulmer, A. J. M. Miller, N. H. Sherden, H. E. Gottlieb, A. Nudelman, B. M. Stoltz, J. E. Bercaw, K. I. Goldberg, *Organometallics* **2010**, *29*, 2176-2179.
- [5] J. Brooks, Y. Babayan, S. Lamansky, P. I. Djurovich, I. Tsyba, R. Bau, M. E. Thompson, *Inorg. Chem.* **2002**, *41*, 3055-3066.
- [6] C. O'Brien, M. Y. Wong, D. B. Cordes, A. M. Z. Slawin, E. Zysman-Colman, *Organometallics* **2015**, *34*, 13-22.
- [7] E. C. Constable, A. Thompson, T. A. Lease, D. G. F. Reese, D. A. Tocher, *Inorg. Chim. Acta* **1991**, *182*, 93-100.
- [8] K. Hanson, A. Tamayo, V. V. Diev, M. T. Whited, P. I. Djurovich, M. E. Thompson, *Inorg. Chem.* **2010**, *49*, 6077-6084.
- [9] C. Bronner, S. A. Baudron, M. W. Hosseini, C. A. Strassert, A. Guenet, L. De Cola, *Dalton Trans.* **2010**, *39*, 180-184.